

## A New Adaptive GMRES Algorithm for Achieving High Accuracy

Maria Sosenkina<sup>1\*</sup>, Layne T. Watson<sup>1</sup>, Rakesh K. Kapania<sup>2</sup> and Homer F. Walker<sup>3</sup>

<sup>1</sup>*Departments of Computer Science and Mathematics, Virginia Polytechnic Institute and State University, Blacksburg, VA 24061-0106, U.S.A.*

<sup>2</sup>*Department of Aerospace and Ocean Engineering, Virginia Polytechnic Institute and State University, Blacksburg, VA 24061-0203, U.S.A.*

<sup>3</sup>*Department of Mathematical Sciences, Worcester Polytechnic Institute, Worcester, MA 01609-2280, U.S.A.*

GMRES( $k$ ) is widely used for solving nonsymmetric linear systems. However, it is inadequate either when it converges only for  $k$  close to the problem size or when numerical error in the modified Gram–Schmidt process used in the GMRES orthogonalization phase dramatically affects the algorithm performance. An adaptive version of GMRES( $k$ ) which tunes the restart value  $k$  based on criteria estimating the GMRES convergence rate for the given problem is proposed here. This adaptive GMRES( $k$ ) procedure outperforms standard GMRES( $k$ ), several other GMRES-like methods, and QMR on actual large scale sparse structural mechanics postbuckling and analog circuit simulation problems. There are some applications, such as homotopy methods for high Reynolds number viscous flows, solid mechanics postbuckling analysis, and analog circuit simulation, where very high accuracy in the linear system solutions is essential. In this context, the modified Gram–Schmidt process in GMRES can fail causing the entire GMRES iteration to fail. It is shown that the adaptive GMRES( $k$ ) with the orthogonalization performed by Householder transformations succeeds whenever GMRES( $k$ ) with the orthogonalization performed by the modified Gram–Schmidt process fails, and the extra cost of computing Householder transformations is justified for these applications. © 1998 John Wiley & Sons, Ltd.

**KEY WORDS** GMRES method; Krylov subspace methods; nonsymmetric linear systems; homotopy curve tracking; sparse matrix

---

\* Correspondence to Maria Sosenkina, Departments of Computer Science and Mathematics, Virginia Polytechnic Institute and State University, Blacksburg, VA 24061-0106, U.S.A.

Contract grant sponsor: Department of Energy; Contract grant numbers: DE-FG05-88ER25068; DE-FG03-94ER25221. Contract grant sponsor: National Aeronautics and Space Administration; Contract grant number: NAG-1-1562. Contract grant sponsor: National Science Foundation; Contract grant numbers: DMS-9625968; DMS-9400217; DMS-9727128. Contract grant sponsor: Air Force Office of Scientific Research; Contract grant numbers: F49620-92-J-0236; F49620-96-I-0089.

## 1. Introduction

Computational challenges of the contemporary world make iterative methods significant ‘team players’ in a sophisticated problem solving process, the overall success of which largely depends on linear system solutions. In the context of homotopy zero curve tracking algorithms [23], for example, to locate the difficult parts of the curve (sharp turning points) a linear system solution in the correction phase of the stepping algorithm along the curve has to be very accurate. In this paper, the ability of the generalized minimal residual algorithm (GMRES) [19] to deal successfully with matrices of varying difficulty and to give high accuracy solutions is investigated.

High accuracy computation is known to be especially important for some circuit design and simulation problems, which involve nonsymmetric unstructured matrices [17]. These problems have proven to be very difficult for any iterative method, and presently, only specially tailored direct methods are used to solve them in a production environment. The impact of numerical error is shown here to be significant in the postbuckling stability analysis of structures which exhibit snap-back and snap-through phenomena. A postbuckling analysis amounts to tracking what is called an equilibrium curve, involving the solution of linear systems with (tangent stiffness) matrices that vary along the equilibrium curve. Mathematically, the snap-back and snap-through behavior of structures correspond to symmetric, structured, and strongly indefinite tangent stiffness matrices, which can be difficult for Krylov subspace iterative methods. Along some portions of the curve the tangent stiffness matrices may be well conditioned and positive definite—easy for iterative methods. This wide variation in linear system difficulty clearly suggests an adaptive strategy. With good preconditioning, the details of an iterative solver become less important, and for many real problems good preconditioning strategies (e.g., multigrid) are available. For some classes of problems, like analog DC circuit design and structural postbuckling stability analysis, good preconditioning strategies are not known, and subtle implementation details of iterative algorithms become paramount.

Section 2 develops the proposed subspace enlarging strategy for GMRES( $k$ ) and addresses some technical issues of the GMRES implementation. Section 3 describes algorithms and realistic test problems for numerical experiments. The numerical results are presented and discussed in Section 4, and Section 5 concludes.

## 2. An implementation of the adaptive GMRES( $k$ ) algorithm

The GMRES algorithm [19] is used for solving a linear system  $Ax = b$  with an  $n \times n$  nonsymmetric invertible coefficient matrix  $A$ . Similar to the classical conjugate gradient method, GMRES produces approximate solutions  $x_j$  which are characterized by a minimization property over the Krylov subspaces  $K(j, A, r_0) \equiv \text{span}\{r_0, Ar_0, A^2r_0, \dots, A^{(j-1)}r_0\}$ , where  $r_0 = b - Ax_0$  and  $j$  is the iteration number. However, unlike the conjugate gradient algorithm, the work and memory required by GMRES grow proportionately to the iteration number, since GMRES needs all  $j$  vectors to construct an orthonormal basis of  $K(j, A, r_0)$ . In practice, the restarted version GMRES( $k$ ) is used, where the algorithm is restarted every  $k$  iterations, taking  $x_k$  as the initial guess for the next cycle of  $k$  iterations, until the residual norm is small enough. Pseudocode for GMRES( $k$ ) is:

```

choose  $x, tol$ 
 $r := b - Ax$ ;
do while  $\|r\| > tol$ 
   $v_1 := r/\|r\|$ ;
  for  $j = 1$  step 1 until  $k$  do
    for  $i = 1$  step 1 until  $j$  do  $h_{i,j} := (Av_j)^T v_i$  end do

     $\tilde{v}_{j+1} := Av_j - \sum_{i=1}^j h_{i,j} v_i$ ;
     $h_{j+1,j} := \|\tilde{v}_{j+1}\|$ ;    if  $h_{j+1,j} = 0$  then goto L1;
     $v_{j+1} := \tilde{v}_{j+1} / h_{j+1,j}$ ;
    compute  $\|r_{j+1}\|$  as described in [19];
    if  $\|r_{j+1}\| \leq tol$  then goto L1
  end do
L1:   $e_1 := (1, 0, \dots, 0)^T$ ;     $V_j := [v_1, \dots, v_j]$ ;
    solve  $\min_y \| \|r\| e_1 - \bar{H}_j y \|$  for  $y_j$  where  $\bar{H}_j$  satisfies  $AV_j = V_{j+1} \bar{H}_j$ ;
     $x := x + V_j y_j$ ;     $r := b - Ax$ 
end do

```

In practice, the modified version of the Gram–Schmidt process is used in the construction of an orthonormal basis for the Krylov subspace. The disadvantage of the restarted version is that it may stagnate and never reach the solution, at least in an allowable amount of time. The essence of the adaptive GMRES strategy proposed here is to adapt the parameter  $k$  to the problem, similar in spirit to how a variable order ODE algorithm tunes the order  $k$ . Joubert [13] proposed an adaptive GMRES strategy that is more expensive and based on different test criteria than that proposed here. With FORTRAN 90, which provides pointers and dynamic memory management, dealing with the variable storage requirements implied by varying  $k$  is not too difficult. The parameter  $k$  can be both increased and decreased—an increase-only strategy is described next followed by pseudocode.

The new adaptive implementation of GMRES( $k$ ) proposed here employs a stagnation test for insufficient residual norm reduction over a cycle of  $k$  steps. In this, GMRES( $k$ ) is declared to have stagnated and the iteration is aborted if at the average rate of progress over the last restart cycle of  $k$  steps, the residual norm tolerance cannot be met in some large multiple ( $bgv$ ) of the remaining number of steps allowed ( $itmax$  is a bound on the number of steps permitted). This estimated number of steps to achieve convergence is called  $test$  in the pseudocode below. Slow progress of GMRES( $k$ ), which indicates that an increase in the restart value  $k$  may be beneficial [21], is detected with a similar test. This near-stagnation test uses a different, smaller multiple ( $smv$ ) of the remaining allowed number of steps. If near-stagnation occurs, the restart value  $k$  is incremented by some value  $m$  and the *same* restart cycle continues. Restarting would mean repeating the non-productive iterations that previously resulted in stagnation, at least in the case of complete stagnation (no residual reduction at all). Such incrementing is used whenever needed if the restart value  $k$  is less than some maximum value  $kmax$ . When the maximum value  $kmax$  is reached, adaptive

GMRES( $k$ ) proceeds as GMRES( $kmax$ ). The values of the parameters  $smv$ ,  $bgv$ , and  $m$  are established experimentally and can remain unchanged for most problems.

The convergence of GMRES may also be seriously affected by roundoff error, which is especially noticeable when a high accuracy solution is required. The orthogonalization phase of GMRES is susceptible to numerical instability. Let  $Q$  be a matrix whose columns are obtained by orthogonalizing the columns of a matrix  $M$ , and define the error matrix  $E = Q^T Q - I$ . The error matrices  $E_{MGS}$ ,  $E_{HR}$  using the modified Gram–Schmidt and Householder reflection methods, respectively, to construct  $Q$  from  $M$  satisfy [3]

$$\|E_{MGS}\|_2 \sim \mathbf{u} \operatorname{cond}(M), \quad \|E_{HR}\|_2 \sim \mathbf{u}$$

where  $\mathbf{u}$  is the machine unit roundoff. Clearly the orthogonalization with Householder reflections is more robust. The GCG-MR and GCG-OR methods of Axelsson and Nikolova [2] are an alternative approach to controlling roundoff error. An implementation of GMRES( $k$ ) using Householder reflections and its block version are given in [22]. (The convergence properties of the block version on the test problems here are no better than those of the point version, and so block versions are not considered further here.) In theory, the implementation of GMRES using Householder reflections is about twice as expensive as when modified Gram–Schmidt is used, at least in terms of expense other than matrix–vector products. However, the Householder reflection method produces a more accurate orthogonalization of the Krylov subspace basis when the basis vectors are nearly linearly dependent and the modified Gram–Schmidt method fails to orthogonalize the basis vectors; this can result in fewer GMRES iterations compensating for the higher cost per iteration using Householder reflections. Let  $e_j$  be the  $j$ th standard basis vector and all norms the 2-norm. Pseudocode for an adaptive version of GMRES( $k$ ) with orthogonalization via Householder reflections implemented as in [22] follows (call this algorithm AGMRES( $k$ )):

```

choose  $x, itmax, kmax, m$ ;
 $r := b - Ax$ ;     $itno := 0$ ;     $cnmax := 1/(50\mathbf{u})$ ;
 $xtol := \max\{100.0, 1.01\mathit{avnz}\}\mathbf{u}$ ;     $tol := \max\{\|r\|, \|b\|\}xtol$ ;
do while  $\|r\| > tol$ 
     $r^{\text{old}} := r$ ;
    determine the Householder transformation matrix  $P_1$ 
        such that  $P_1 r = \pm \|r\| e_1$ ;
     $k_1 = 1$ ;     $k_2 = k$ ;
L1: for  $j := k_1$  step 1 until  $k_2$  do
     $itno := itno + 1$ ;
     $v := P_j \cdots P_1 A P_1 \cdots P_j e_j$ ;
    determine  $P_{j+1}$  such that  $P_{j+1} v$  has zero components
        after the  $(j + 1)$ st;
    compute  $\|r_{j+1}\|$  as described in [19];
    estimate condition number  $\operatorname{cond}(A V_j)$  of GMRES least squares
        problem via the incremental condition number  $ICN$  by

```

```

DLAIC1 from LAPACK where  $V_j = [P_1 e_1, \dots, P_1 \cdots P_j e_j]$ ;
if  $ICN > cnmax$  then abort;
if  $\|r_{j+1}\| \leq tol$  then goto L2
end do
 $test := k_2 \times \log [tol/\|r\|] / \log \left[ \|r\| / \left( (1.0 + 10u) \|r^{old}\| \right) \right]$ ;
if  $k_2 \leq kmax - m$  and  $test \geq smv \times (itmax - itno)$  then
     $k_1 := k_2 + 1;$      $k_2 := k_2 + m;$ 
    goto L1
end if
L2:  $e_1 := (1, 0, \dots, 0)^T;$      $k := k_2;$ 
    solve  $\min_y \| \|r\| e_1 - \bar{H}_j y \|$  for  $y_j$  where  $\bar{H}_j$  satisfies  $AV_j = V_{j+1} \bar{H}_j$ ;
     $q := \begin{pmatrix} y_j \\ 0 \end{pmatrix};$      $x := x + P_1 \cdots P_j q;$      $r := b - Ax;$ 
    if  $\|r\| \leq tol$  then exit;
    if  $\|r^{old}\| < \|r\|$  then
        if  $\|r\| < tol^{2/3}$  then
            exit
        else
            abort
        end if
    end if
     $test := k \times \log [tol/\|r\|] / \log \left[ \|r\| / \left( (1.0 + 10u) \|r^{old}\| \right) \right]$ ;
    if  $test \geq bgv \times (itmax - itno)$  then
        abort
    end if
end do

```

The rounding error of a sparse matrix–vector multiplication depends on only the non-zero entries in each row of the sparse matrix, so the error tolerance  $xtol$  is proportional to the average number of nonzeros per row  $avnz = (\text{number of nonzeros in } A)/n$ . In most applications, the initial estimate  $x_0 = 0$ ; however, this is certainly not the case for homotopy zero curve tracking, where the previous tangent vector provides a good estimate  $x_0$ . Since GMRES convergence is normally measured by reduction in the initial residual norm, the convergence tolerance is  $tol = \max\{\|r_0\|, \|b\|\}xtol$ .

A possible symptom of AGMRES( $k$ ) going astray is an increase in the residual norm between restarts (the residual norm is computed by direct evaluation at each restart). If the residual norm on the previous restart is actually smaller than the current residual norm, then AGMRES( $k$ ) terminates (this happened often on the test problems in Sections 3.1–3.3). The solution is considered acceptable if  $\|r\| < tol^{2/3}$ , although this loss of accuracy may cause the client algorithm (the ‘outer’ algorithm requiring solutions to linear systems) to work harder or fail. A robust client algorithm can deal gracefully with a loss of accuracy in

the linear system solutions. If  $\|r\| \geq tol^{2/3}$ , AGMRES( $k$ ) is deemed to have failed. In this latter case, the continuation of GMRES( $k$ ) would typically result in reaching a limit on the number of iterations allowed and a possible repetition of  $\|r^{old}\| < \|r\|$  in later restarts. This admittedly *ad hoc* choice of  $tol^{2/3}$  avoided failures for AGMRES( $k$ ) for all test problems. AGMRES( $k$ ) may exceed an iteration limit when it is affected by roundoff errors in the case of a (nearly) singular GMRES least-squares problem. The condition number of the GMRES least-squares problem is monitored by the incremental condition estimate [2] as in [4]. AGMRES( $k$ ) aborts when the estimated condition number is greater than  $1/(50\mathbf{u})$ .

### 3. Numerical experiments

A comparative study of the proposed adaptive version of GMRES( $k$ ) considers some other versions of GMRES( $k$ ): the standard implementation of GMRES( $k$ ) [19], the adaptive GMRES( $k$ ) with modified Gram–Schmidt orthogonalization, GMRES( $k$ ) with GMRES-ILU(0) preconditioning [18], and the popular iterative method QMR [7]. A brief description of the GMRES( $k$ ) with GMRES-ILU(0) preconditioning and QMR algorithms follows.

The *GMRES( $k$ ) with GMRES-ILU(0) preconditioning* method is a variation of flexible GMRES developed in [18]. Flexible GMRES( $k$ ) differs from the standard preconditioned GMRES( $k$ ) implementation by allowing variations in preconditioning at each iteration. Let  $M_i$  be the computed preconditioner at the  $i$ th iteration. Then an iterate  $x_k$  is given by

$$x_k = x_0 + \left[ M_1^{-1}v_1, \dots, M_k^{-1}v_k \right] y_k$$

where  $y_k$  is the solution to the GMRES least-squares problem and the  $v_i$  are the same as in the standard GMRES( $k$ ). Here the application of  $M_i$  corresponds to an ‘inner’ iteration consisting of  $\tilde{k} \ll k$  steps of an ILU(0) preconditioned GMRES and with the iteration limit  $itmax \ll itmax$ .

The *quasi-minimal residual* method QMR [7] is based on a modification of the classical nonsymmetric Lanczos algorithm. Given two starting vectors  $v_1$  and  $w_1$ , the Lanczos algorithm uses three-term recurrences to generate sequences  $\{v_i\}_{i=1}^L$  and  $\{w_i\}_{i=1}^L$  of vectors satisfying

$$\begin{aligned} \text{span}\{v_1, \dots, v_m\} &= \text{span}\{v_1, Av_1, \dots, A^{m-1}v_1\} \\ \text{span}\{w_1, \dots, w_m\} &= \text{span}\{w_1, A^T w_1, \dots, (A^T)^{m-1}w_1\} \end{aligned}$$

for  $m = 1, \dots, L$ , and  $w_i^T v_j = d_i \delta_{ij}$ , with  $d_i \neq 0$ , for all  $i, j = 1, \dots, L$ , where  $\delta_{ij}$  is the Kronecker delta.

An implementation of QMR based on the look-ahead Lanczos process avoids most breakdowns associated with Lanczos-type algorithms [6]. At the  $k$ th iteration, QMR computes an iterate  $x_k$  as

$$x_k = x_0 + V^{(k)}z$$

where the columns of the matrix  $V^{(k)}$  are the right look-ahead Lanczos vectors  $v_1, \dots, v_k$ , and the vector  $z$  is the unique minimizer of

$$\left\| \|r_0\|e_1 - H_e^{(k)}z \right\|$$

where  $H_e^{(k)}$  is a  $k \times k$  block tridiagonal matrix augmented with a row of the form  $\rho e_k^T$ .

Based on the conclusions of [5, 12, 15] *incomplete LU factorization* with zero fill in (ILU(0)) and *Gill–Murray* preconditioning are considered for nonsymmetric unstructured and symmetric skyline structured matrices, respectively. Let  $Z \subset \{(i, j) \mid 1 \leq i, j \leq n, i \neq j\}$  be a subset of the set of indices where the matrix  $A$  has zeros. Then the ILU factorization of  $A$  is given by  $Q = LU$ , where  $L$  and  $U$  are lower triangular and unit upper triangular matrices, respectively, satisfying

$$\begin{aligned} L_{ij} &= U_{ij} = 0, & \text{for } (i, j) \in Z \\ Q_{ij} &= A_{ij}, & \text{for } (i, j) \notin Z, i \neq j \\ Q_{ii} &= A_{ii}, & \text{whenever possible} \end{aligned}$$

The factors of the preconditioning matrix  $Q$  preserve the sparsity pattern of  $A$ . The Gill–Murray preconditioner [8] for a matrix  $A$  with a skyline sparsity pattern is a positive definite approximation  $Q = GG^T$  to  $A$ . The lower triangular matrix  $G$  has the same skyline structure as  $A$ , and is chosen such that  $G$  is always well conditioned.

For future reference the considered algorithms will be called:

- AGH — adaptive restarted GMRES with Householder reflections in the orthogonalization phase;
- AGS — adaptive restarted GMRES with modified Gram–Schmidt in the orthogonalization phase;
- FGS — flexible restarted GMRES with  $\tilde{k} = k/3, \widetilde{itmax} = itmax/20$ ;
- GS — standard implementation of restarted GMRES;
- Q — three-term recursion QMR.

### 3.1. Circuit design and simulation

The circuit simulation test problems considered here are from [15] and [17], and are representative of full-scale commercial design at AT&T Bell Laboratories. The DC operating point problem is typically formulated as a system of  $n$  equations in  $n$  unknowns, i.e.,  $F(x) = 0$ , where  $F : E^n \rightarrow E^n$ , and  $E^n$  is  $n$ -dimensional real Euclidean space. The unknowns are voltages and branch currents and the equations represent the application of Kirchoff's current and voltage laws at various points in the circuit. Different circuit components (resistor, transistor, diode, etc.) impose linear and nonlinear relations among the unknowns. In present fabrication technologies, circuit components are arranged in the form of a graph that is almost planar, which limits the density of interconnections between circuit elements, leading to a sparse Jacobian matrix. Figure 1 shows one of the circuits (Brokaw voltage reference [17], 'vref') from which the test problems were derived.

Except for rather special cases, circuit equations lead to large nonsymmetric unstructured matrix problems. In some cases, a circuit element like a transistor is replicated as a small 'subcircuit', which is installed in place of every transistor in the network. This policy results in a replication of structurally identical submatrices throughout the overall system Jacobian matrix. The sparsity pattern for the Jacobian matrix corresponding to one of the test circuits (bgatt) with the diagonal blocks corresponding to the transistor subcircuits is shown in Figure 2.

For each test problem, the various iterative methods were applied to a sequence of Jacobian matrices obtained along a homotopy zero curve for that problem. For the rest of the test problems described below, the iterative methods were actually implemented as

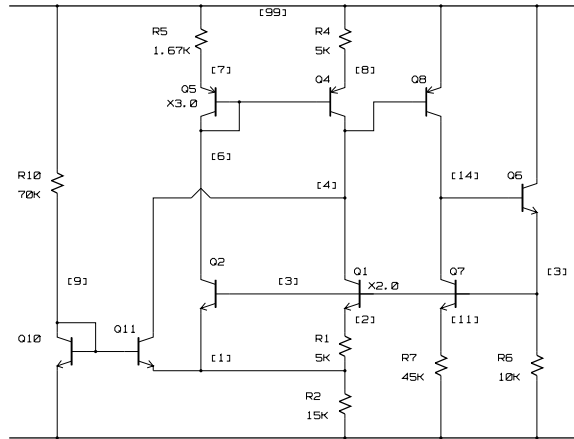


Figure 1. Circuit diagram for the circuit 'vref'



Figure 2. Jacobian matrix sparsity pattern corresponding to the circuit 'bgatt'



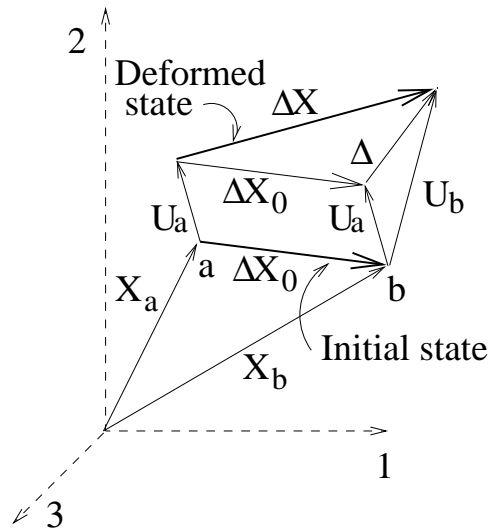


Figure 3. Space truss element

subroutines within the homotopy curve tracking software HOMPACk [25]. Specifically a FORTRAN 90 version of the normal flow subroutine FIXPNS was used, resulting in the  $(n + 1) \times (n + 1)$  linear systems described in [12]—note that these are slightly different from the linear systems for the sparse normal flow algorithm given in [25].

### 3.2. Space truss stability analysis

The stability characteristics of a space truss under multiple independent loads are described in [11]. A brief derivation of the nonlinear equilibrium equations, whose solution by a homotopy method generates the linear systems to be solved, is given here.

#### 3.2.1. Finite element model

The axial deformation of the truss element in Figure 3 is  $e = L - L_0$ , where  $L_0$  and  $L$  are the element lengths in the initial and deformed states, respectively. It follows from Figure 3 that

$$L = \|\Delta X\| = \left( \sum_{j=1}^3 L_j^2 \right)^{1/2}, \quad L_0 = \|\Delta X_0\| = \left( \sum_{j=1}^3 L_{0j}^2 \right)^{1/2},$$

$$L_j = L_{0j} + \Delta_j, \quad \Delta X_0 = X_b - X_a, \quad \Delta = U_b - U_a, \quad \Delta X = \Delta X_0 + \Delta$$

where  $X_a, X_b$  are the initial coordinate vectors at the  $a, b$ -end of the element;  $U_a, U_b$  are the global displacement vectors at the  $a, b$ -end of the element; and the vectors  $\Delta X_0, \Delta X$  coincide with the initial, deformed state of the element. The strain energy of the element is

$$\pi = \frac{1}{2} \gamma_0 e^2$$

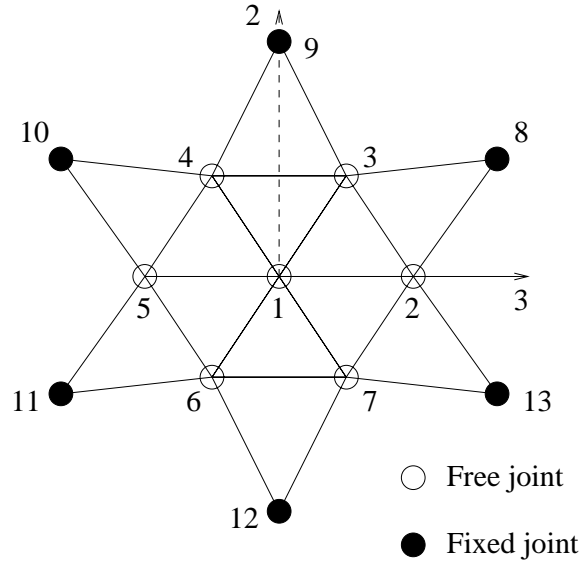


Figure 4. Lamella dome (21-degree-of-freedom)

where  $\gamma_0 = EA/L_0$  is the extensional stiffness of the element,  $E$  is Young’s modulus of elasticity, and  $A$  is the cross sectional area of the truss element. The principle of virtual work yields the equation of equilibrium

$$F(q, \lambda, \bar{Q}) = -\lambda \bar{Q} + \sum_{i=1}^m R^i = 0$$

where  $q$  is the generalized displacement vector,  $\lambda$  is the scalar load parameter,  $\bar{Q}$  is the load distribution vector, the vector function  $F$  is the force imbalance, and

$$R_k^i = \frac{\partial \pi^i}{\partial q_k}, \quad \text{for } k = 1, 2, \dots, n$$

The superscript  $i$  identifies the  $m$  elements of the assemblage. The  $n \times (n + 1)$  Jacobian matrix becomes

$$DF = [K, -\bar{Q}], \quad \text{where } K = \sum_{i=1}^m K^i, \quad K^i = \left[ \frac{\partial^2 \pi^i}{\partial q_k \partial q_l} \right]$$

$K^i$  is the tangent stiffness matrix of the element  $i$  expressed relative to the generalized displacements of the assemblage. It is computed by the code number method [24] from the global stiffness matrix of element  $i$ .

### 3.2.2. Structure 1

Figure 4 shows a 21-degree-of-freedom lamella dome. The joints lie on the surface of a spherical cap with a radius of 157.25 inches. The support ring of the cap has a radius of 50 inches. All joints are located so that the structure is symmetric about the global  $x_1$ -axis

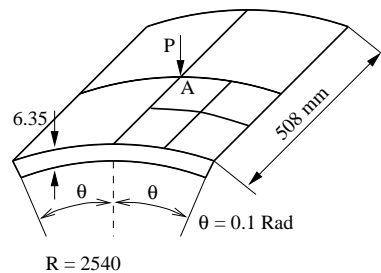


Figure 5. Cylindrical shell geometry; load applied at A

which extends down vertically through the apex. The six support joints are fixed in all three directions. Each member of the structure has a cross-sectional area of 0.18 square inches and an elastic modulus of 2 900 ksi. The structure is subjected to a vertical load at the apex.

### 3.2.3. Structure 2

This is another lamella dome with a tension ring at the base having 69 degrees of freedom, similar to Structure 1 but with a different geometrical arrangement of the free joints, different joint constraints, and an unsymmetric loading pattern [11]. The effect of modeling a space truss with truss elements in concentric rings is that changing the number of truss elements changes the model and its behavior. Thus the dome problems with different degrees of freedom considered here are qualitatively different, with different buckling loads.

### 3.3. Shallow shell stability analysis

Another test problem is the finite element analysis of a shallow cylindrical shell (Figure 5) under a concentrated load [26]. The shell shown in Figure 5 is hinged at the longitudinal edges and free along the curved boundaries.

The structure exhibits snap-through as well as snap-back phenomena, with horizontal and vertical tangents. A finite element model based on a curved quadrilateral 48-degree-of-freedom thin-shell element (Figure 6) is used to form the equations of equilibrium [14]. The element has four corner nodes and each node has 12 degrees of freedom. Figure 6 shows the undeformed middle surface of the shell element embedded in a fixed Cartesian coordinate system  $x^i$  ( $i = 1, 2, 3$ ). The Cartesian coordinates  $x^i$  ( $i = 1, 2, 3$ ) of the middle surface are modeled by polynomial functions of the curvilinear co-ordinates  $\xi$  and  $\eta$  with a total of  $N$  terms:

$$x^i(\xi, \eta) = \sum_{j=1}^N C_j^i \xi^{m_j} \eta^{n_j}$$

where the constants  $m_j$  and  $n_j$  define the powers of  $\xi$  and  $\eta$ , respectively, for the  $j$ th term. The constants  $C_j^i$  are solved for based on the coordinates  $x_j$  at  $N$  selected points. Precisely, bicubic Hermite polynomials in the curvilinear coordinates  $\xi$  and  $\eta$  are used as basis functions for the interpolating polynomial.

The Cartesian coordinates of a given point are described by a system of parametric equations

$$x^i = f^i(\theta^1, \theta^2)$$

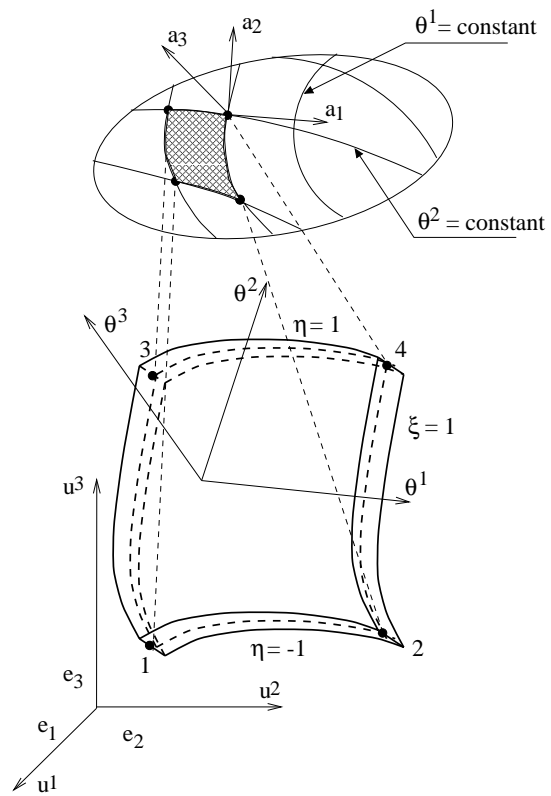


Figure 6. Thin-shell element coordinate system

where the parameters  $\theta^\alpha$  ( $\alpha = 1, 2$ ) serve as coordinates on the surface and can be regarded as an arbitrary selected system.

The two base vectors  $a_1$  and  $a_2$  are obtained as derivatives of  $f$  with respect to each component  $\theta^\alpha$ :

$$a_\alpha = \frac{\partial f^i}{\partial \theta^\alpha} e_i = f_\alpha^i e_i$$

where the  $e_i$  are the standard basis vectors, and tensor notation is being employed. The unit normal  $a_3$  to the surface is given as

$$a_3 = \frac{a_1 \times a_2}{|a_1 \times a_2|} = n^i e_i$$

where  $n^i = c e_{ijk} f_1^j f_2^k$ ,  $e_{ijk}$  is the alternating symbol,  $c = 1/|a_1 \times a_2| = 1/\sqrt{a}$ ,

$$a = \begin{vmatrix} a_{11} & a_{12} \\ a_{21} & a_{22} \end{vmatrix}, \quad a_{\alpha\beta} = a_\alpha \cdot a_\beta = f_\alpha^i f_\beta^i$$

The metric tensor  $a_{\alpha\beta}$  yields the first fundamental form of a surface  $ds^2 = a_{\alpha\beta} d\theta^\alpha d\theta^\beta$ , where  $ds$  is the distance between two neighboring points at  $\theta^\alpha$  and  $\theta^\alpha + d\theta^\alpha$  ( $\alpha = 1, 2$ ). The curvature tensor  $b_{\alpha\beta}$  is given as

$$b_{\alpha\beta} = n^i \frac{\partial^2 f^i}{\partial \theta^\alpha \partial \theta^\beta} = n^i f_{\alpha\beta}^i$$

After deformation, the same point has Cartesian coordinates  $\bar{f}^i = f^i + u^i$ , where  $u^i$  ( $i = 1, 2, 3$ ) are the Cartesian components of the displacement vector. The 12 degrees of freedom for each node are  $u^i, u_1^i, u_2^i, u_{12}^i$  ( $i = 1, 2, 3$ ). In the deformed state, the metric and curvature tensors take the form

$$\bar{a}_{\alpha\beta} = (f^i + u^i)_\alpha (f^i + u^i)_\beta = \bar{f}_\alpha^i \bar{f}_\beta^i, \quad \bar{b}_{\alpha\beta} = \bar{n}^i \bar{f}_{\alpha\beta}^i$$

where

$$\bar{n}^i = (\bar{a})^{-1/2} e_{ijk} \bar{f}_1^j \bar{f}_2^k, \quad (\bar{a})^{-1/2} \approx (a)^{-1/2} (1 - A/a) \\ A = (\varepsilon_{11} a_{22} + \varepsilon_{22} a_{11} - 2\varepsilon_{12} a_{12})$$

The tangential strain measure  $\varepsilon_{\alpha\beta}$  is given as

$$\varepsilon_{\alpha\beta} = \frac{1}{2} (\bar{a}_{\alpha\beta} - a_{\alpha\beta}) = \frac{1}{2} (f_\alpha^i u_\beta^i + f_\beta^i u_\alpha^i + u_\alpha^i u_\beta^i), \quad i = 1, 2, 3$$

The curvature strain measure  $\kappa_{\alpha\beta}$  is given as

$$\kappa_{\alpha\beta} = -(\bar{b}_{\alpha\beta} - b_{\alpha\beta}) + \frac{1}{2} (b_\alpha^\delta \varepsilon_{\beta\delta} + b_\beta^\delta \varepsilon_{\alpha\delta})$$

where  $b_\alpha^\delta$  is defined in terms of the contravariant tensor  $a^{\beta\delta}$  by  $b_\alpha^\delta = b_{\alpha\beta} a^{\beta\delta}$ .

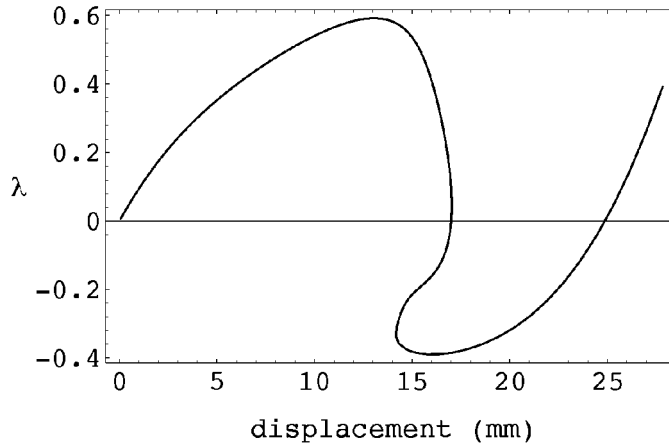


Figure 7. Load factor  $\lambda$  versus displacement  $u^3$  at the point A for the shell in Figure 5

The total potential energy of the model can be written as

$$\Pi_p(u) = \int_A \int [W(\varepsilon_{\alpha\beta}(u), \kappa_{\alpha\beta}(u)) - p^i u^i] \sqrt{a} \, d\theta^1 d\theta^2$$

where  $W$  is the strain energy density per undeformed middle surface unit of the shell,  $p^i$  ( $i = 1, 2, 3$ ) are the Cartesian components of the externally applied load, and  $u^i$  ( $i = 1, 2, 3$ ) are the Cartesian components of the displacement vector. The strain energy  $W$  is given by

$$W = \frac{1}{2} H^{\alpha\beta\lambda\mu} \left( \varepsilon_{\alpha\beta} \varepsilon_{\lambda\mu} + \frac{h^2}{12} \kappa_{\alpha\beta} \kappa_{\lambda\mu} \right)$$

where  $h$  is the thickness of the shell. The tensor of elastic moduli  $H^{\alpha\beta\lambda\mu}$  is defined as

$$H^{\alpha\beta\lambda\mu} = \frac{Eh}{2(1+\nu)} \left[ a^{\alpha\lambda} a^{\beta\mu} + a^{\alpha\mu} a^{\beta\lambda} + \frac{2\nu}{1-\nu} a^{\alpha\beta} a^{\lambda\mu} \right]$$

where  $E$  is Young's modulus,  $\nu$  is Poisson's ratio,  $a^{\alpha\beta} a_{\lambda\beta} = \delta_{\alpha\lambda}$  defines the contravariant tensor  $a^{\alpha\beta}$ , and  $\delta_{\alpha\lambda}$  is the Kronecker symbol.

The equilibrium equations of the model are obtained by setting the variation  $\delta \Pi_p(u)$  to zero, or equivalently

$$\nabla \Pi = 0$$

The Jacobian matrix of the equilibrium equations is obtained by finite difference approximations.

By symmetry, only a quarter of the shell is modeled using a  $2 \times 2$  mesh. The material properties are  $\nu = 0.3$  and  $E = 3.101 \text{ kN/mm}^2$ . An initial external concentrated load of 0.2 kN is applied. The equilibrium curve (load factor  $\lambda$  versus displacement at the point A) of the cylindrical shell is shown in Figure 7, where the actual load is 0.2λ kN.

#### 4. Results

Tables 1–6 show the iteration counts and timing results for adaptive GMRES( $k$ ) with modified Gram–Schmidt and Householder reflection orthogonalization procedures (AGS, AGH respectively) and different subspace increment values  $m$ , standard GMRES( $k$ ) (GS), flexible GMRES( $k$ ) (FGS), and QMR (Q). The notation AGH:2, for example, means AGH with  $m = 2$ . Each of the iterative methods was applied to all of the test problems. An iterative solver is deemed to have converged when the relative residual norm reduction is less than  $\max\{100, \text{avnz}\}\mathbf{u}$ . The limit on the number of iterations is  $30n$ . This number is quite reasonable for moderate size realistic problems to be solved on modern computer hardware, although for very large  $n$  a limit like  $30\sqrt{n}$  is more appropriate. (Note from Tables 1–3 that  $30\sqrt{n}$  does not suffice here.) This iteration limit requires explanation. First, ideally convergence should occur in far fewer iterations than  $n$ , and for well preconditioned PDE problems this usually occurs. However, for other classes of problems and for mediocre preconditioners, more than  $n$  iterations may be required, and permitting  $30n$  iterations is preferable to permitting very large subspace dimensions  $k$  or permitting failure of the linear system solution server to return an accurate solution to the client homotopy algorithm. Second, low accuracy might be acceptable if only Newton corrections were being computed (although inaccurate Newton steps will wreak havoc on homotopy path step size control algorithms), but inaccurate tangents may result in losing the path or in very small, inefficient steps near extremely sharp turns of the homotopy path. Clearly high accuracy is not required *everywhere* along the homotopy path, and effectively adjusting the linear system solution accuracy along the homotopy path, while preserving reliable path step size control, is an open research question.

All reported CPU times are for 64-bit IEEE arithmetic on a DEC Alpha 3000/600 workstation. The average, maximum, and minimum number of iterations per linear system solution along the homotopy zero curve are shown in Tables 1–3. Note that in the FGS column the numbers for the  $x_k$  outer iterations of flexible GMRES( $k$ ) are given. Tables 5 and 6 report the total CPU time in seconds required for an iterative method to obtain all the linear system solutions needed for HOMPACT to track a homotopy zero curve for a certain arc length specified for each problem. For the circuit problems (Table 4), the reported CPU time is the time necessary to solve a certain number of linear systems arising along a portion of the homotopy zero curve.

An asterisk denotes convergence failure, meaning any of the following occurred: (1) desired error tolerance not met after  $30n$  iterations, (2) dangerous near singularity detected for the GMRES least squares problem, (3) residual norm increased between restart cycles and was not small, (4) stagnation occurred for GMRES-like methods. In Tables 1–3, the numbers in parentheses ( $k$ ) show the restart values  $k$  whenever applicable. For AGS and AGH, the notation ( $a \rightarrow b$ ) shows the initial restart value  $a$  and the maximum restart value  $b$  reached by the adaptive strategy anywhere along the homotopy zero curve. Results are shown for FGS and GS in Table 1 for several different restart values.

The initial  $k$  values for the problems are chosen to compare GMRES-like methods when: (1) GMRES( $k$ ) does not exhibit near stagnation behavior at all ( $n = 468$  circuit problem,  $n = 119$  shell problem), (2) near stagnation causes an increase in  $k$  for *all* the matrices along the curve (circuit problem  $n = 125$ ), and (3) near stagnation is detected for *some* matrices along the curve. In the first case, adaptive and nonadaptive GMRES( $k$ ) perform the same. In the second and third cases, GS with  $k$  the same as the initial  $k$  in AGMRES( $k$ ) reaches no final solution, which has a disastrous effect on the outer (client) algorithm calling GS.

Table 1. Average, maximum, and minimum number of iterative solver iterations per linear system along homotopy zero curve for circuit design problems (ILU(0) preconditioner)

$n$	AGH:2	AGH:4	AGH:6	AGS:2	AGS:4	AGS:6	GS	FGS	Q
31	23,112,1 (2 → 6)	19,108,1 (2 → 6)	19,108,1 (2 → 6)	24,112,1 (2 → 6)	19,108,1 (2 → 6)	19,108,1 (2 → 6)	(2) *	(2) *	*
59	52,231,14 (4 → 6)	48,231,14 (4 → 8)	49,231,14 (4 → 10)	53,231,14 (4 → 6)	53,231,14 (4 → 8)	*	(6)12,48,1 (4) *	(3)8,196,1 *	*
67	587,1 150,344 (5 → 15)	557,1 050,339 (5 → 15)	471,734,286 (5 → 15)	576,1 578,291 (5 → 15)	613,1 520,330 (5 → 15)	531,1295,312 (5 → 15)	(10)9,10,7 (5) *	(3) *	*
125	143,193,84 (4 → 6)	121,169,84 (4 → 8)	102,131,82 (4 → 10)	146,230,84 (4 → 6)	122,156,84 (4 → 8)	110,140,73 (4 → 10)	(15)288,359,217 (4) *	(8)20,107,9 (4) *	*
468	623,1842,252 (15 → 15)	623,1 842,252 (15 → 15)	623,1 842,252 (15 → 15)	603,1 740,252 (15 → 15)	603,1 740,252 (15 → 15)	603,1 740,252 (15 → 15)	(10)83,110,49 (15)603,1 740,252	(6)62,142,9 *	*
1854	2 719,4 340,1 173 (35 → 47)	2 768,4 234,956 (35 → 47)	2 419,3 953,874 (35 → 47)	2 710,4 165,1 347 (35 → 47)	2 725,3 990,1 096 (35 → 47)	2 523,3 947,1 060 (35 → 47)	(35) * (47)611,838,539	*	*



Table 2. Average, maximum, and minimum number of iterative solver iterations per linear system along homotopy curve for thin shell problem (Gill-Murray preconditioner)

$n$	AGH:2	AGH:4	AGH:6	AGS:2	AGS:4	AGS:6	GS	FGS	Q
55	80,1 239,1 (8 → 20)	57,888,1 (8 → 20)	44,748,1 (8 → 24)	*	*	*	*	*	*
119	6,134,1 (5 → 5)	6,134,1 (5 → 5)	6,134,1 (5 → 5)	6,140,1 (5 → 5)	6,140,1 (5 → 5)	6,140,1 (5 → 5)	6,140,1 (5)	*	*
1 239	3,14,1 (12 → 20)	3,14,1 (12 → 20)	3,14,1 (12 → 20)	*	*	*	*	*	*

Table 3. Average, maximum, and minimum number of iterative solver iterations per linear system along homotopy zero curve for lamella dome problem (Gill-Murray preconditioner)

$n$	AGH:2	AGH:4	AGH:6	AGS:2	AGS:4	AGS:6	GS	FGS	Q
21	22,452,1 (4 → 10)	19,536,1 (4 → 12)	16,528,1 (4 → 10)	23,508,1 (4 → 10)	18,387,1 (4 → 12)	*	*	*	*
69	38,1 374,1 (8 → 18)	34,1 347,1 (8 → 18)	35,1 576,1 (8 → 18)	40,1 331,1 (8 → 18)	39,1 442,1 (8 → 18)	*	*	(4) *	*
								(9)3,75,1	

An adaptive strategy is especially useful when the degree of difficulty of linear systems in a sequence varies, and it is hard to predict what value of  $k$  is needed for convergence of GMRES( $k$ ) on all the linear systems. Even for a small shell problem ( $n = 55$ ),  $k$  can vary between 8 and 20, and the number of iterations can vary between a low of 1 and a high of 1 239. The AGH:4 adaptive strategy on one of the matrices from the ‘vref’ circuit is shown in Figure 8, where a circle indicates an increase in the subspace dimension ( $k = 8$  initially). The adaptive strategy is invoked for the first time rather early—to jump off the near-stagnation ‘plateau’ after the 24th iteration. The subspace dimension is increased once more (after 172 iterations), which suggests that AGH:4 has enough vectors to solve the system within the iteration limit. Note that a smaller iteration limit would cause AGH:4 to increase the subspace dimension quicker.

For every circuit problem, GS with  $k$  the maximum restart value produced by the adaptive strategy converges faster than AGS or AGH. However, neither AGS nor GS always converges for the shell problems (Table 2) with  $n = 55, 1\ 239$ , due to the failure of the modified Gram–Schmidt process to accurately orthogonalize the Krylov subspace basis. When the vectors encountered in the orthogonalization process become increasingly nearly linearly

Table 4. Iterative solver execution time in seconds for circuit problems (ILU(0) preconditioner)

$n$	AGH:2	AGH:4	AGH:6	AGS:2	AGS:4	AGS:6	GS	FGS
31	0.66	0.55	0.55	0.40	0.36	0.36	0.18	1.53
59	0.50	0.45	0.46	0.33	0.31	*	0.08	*
67	3.70	3.53	2.96	1.97	2.09	1.82	0.55	11.04
125	1.51	1.34	1.18	0.98	0.81	0.74	0.56	14.56
468	11.45	11.46	11.45	5.39	5.39	5.38	5.32	*
1854	383.60	386.29	338.76	133.17	133.04	123.31	32.98	*

Table 5. Iterative solver execution time in seconds for thin shell problem (Gill-Murray preconditioner)

$n$	AGH:2	AGH:4	AGH:6	AGS:2	AGS:4	AGS:6	GS
55	25.82	19.68	14.53	*	*	*	*
119	2.70	2.71	2.69	2.43	2.42	2.41	2.44
1239	111.40	107.12	100.90	*	*	*	*

Table 6. Iterative solver execution time in seconds for lamella dome problem (Gill-Murray preconditioner)

$n$	AGH:2	AGH:4	AGH:6	AGS:2	AGS:4	AGS:6	FGS
21	2.24	1.89	1.66	1.74	1.39	*	*
69	29.45	25.93	27.27	24.26	23.64	*	38.86

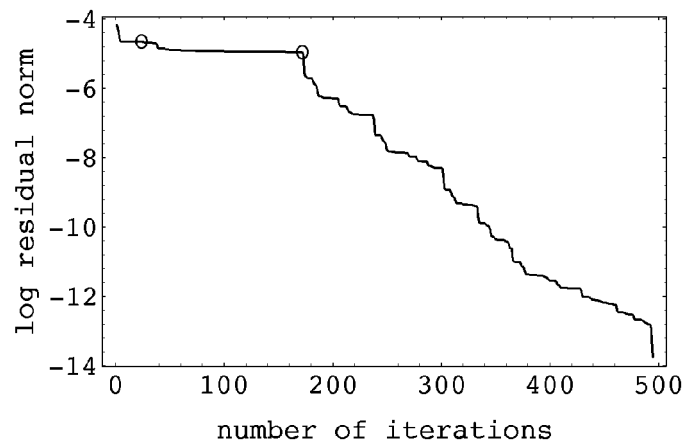


Figure 8. Effect of adaptive strategy on residual norm

dependent, the orthogonalization error of the modified Gram–Schmidt process grows with the number of vectors orthogonalized. For example, AGS:6 fails on all lamella dome problems whereas AGS:2 and AGS:4 succeed (Table 3). The same situation is encountered for the circuit problem with  $n = 59$ . All these failures just mentioned ensue from the estimated condition number of the GMRES least squares problem indicating numerical singularity. AGH successfully passes the condition number test on all the problems, producing a more accurate orthogonal basis for the Krylov subspace.

Table 7 shows the AGS and AGH convergence traces for a typical linear system solution along the equilibrium curve for a thin shell problem. The (preconditioned) matrix  $A$  of this particular linear system has condition number  $1.15 \times 10^{10}$ , inertia  $(4, 0, 52)$ , and smallest eigenvalue  $-8.014$ . Table 7 reports the recursively maintained (computed) GMRES residual, the exact (calculated in 128-bit arithmetic) residual, and the estimated condition number of the GMRES least-squares problem at the end of each iteration for AGS and AGH. The first iteration in each restart cycle is shown in bold face type, and the adaptive strategy was not invoked on this system. There are several observations from Table 7: (1) the performances of AGS and AGH are almost indistinguishable until the exact residual norm becomes smaller than  $\text{cond}(A)\mathbf{u} \approx 2.5 \times 10^{-6}$ , which is consistent with theoretical results in [10]. (2) However, much higher accuracy is consistently achievable by AGH on a wide range of qualitatively different problems (the linear systems along the homotopy zero curves for the problems in Sections 3.1–3.3 are fundamentally different), as proven by the results in Tables 1–6. The right hand sides, coming from nonlinear normal flow iteration corrections, are not ‘special’ in any way whatsoever. (3) When the computed residual norm for AGS reaches  $\mathcal{O}(\text{cond}(A)\mathbf{u})$ , there is a pronounced oscillation of the true residual norm, and stagnation of the computed residual norm. At this point, AGH is behaving differently, producing a computed residual norm small enough to terminate the current restart cycle before the GMRES least-squares problem becomes ill-conditioned enough to trigger the condition number test. This behaviour of AGH relative to AGS, shown in Table 7, occurred consistently on all the test problems where AGS failed. (4) With the condition number test turned off, AGH always reached a higher accuracy solution, but AGS frequently completely stagnated and did not. For this particular linear system, both AGS and AGH converge to a higher accuracy solution, but AGS does so at a cost of more iterations, which is caused by stagnation of its computed residual norm. For larger subspaces, such a stagnation severely impedes the convergence of AGS.

AGH never fails, but at a cost of more CPU time. For example, good candidates for a CPU time comparison (Tables 1 and 4) are AGH:4, AGS:4 for the  $n = 31$  circuit problem and AGH:2, AGS:2 for the  $n = 59$  circuit problem, since they exhibit similar adaptive behavior in terms of iteration counts. In both cases, AGS outperforms AGH only by a factor of 1.5. This factor varies slightly depending on the performance of the adaptive strategy and the orthogonalization accuracy for a particular problem. If the maximum number of AGS iterations is large relative to  $n$  (e.g., the dome problem with  $n = 69$ ), then AGH is only a little slower than AGS (Table 6), but for large  $n$  ( $n = 1854$  circuit problem), AGH is slower than AGS by a factor of 2.8 and also takes more iterations (Tables 1 and 4). When a high accuracy solution is required, it is hard to predict which orthogonalization procedure will lead to the smallest number of iterations. For example, from Table 1, AGH produces a lower maximum number of iterations than AGS for some cases but not all cases.

The number of restart cycles in AGMRES( $k$ ) depends on the increment value  $m$ . Tables 1–3 indicate that even a small increment in the restart value leads to convergence. However, if the increment value is too small, often extra restart cycles are executed, which increases

Table 7. Convergence trace for a typical system from thin shell problem ( $n = 55$ ) comparing AGS with AGH

$j$	AGS:2(25)			AGH:2(25)		
	computed residual	exact residual	cond( $AV_j$ )	computed residual	exact residual	cond( $AV_j$ )
1	<b>9.88233703 + 1</b>	<b>9.88233703 + 1</b>	<b>1.00000000 + 0</b>	<b>9.88 + 1</b>	<b>9.88 + 1</b>	<b>1.00 + 0</b>
2	8.41201033 + 0	8.41201033 + 0	2.71517580 + 3	8.41 + 0	8.41 + 0	2.72 + 3
3	5.30062772 + 0	5.30062772 + 0	3.60300441 + 4	5.30 + 0	5.30 + 0	3.60 + 4
4	6.00276476 - 1	6.00276476 - 1	2.36085135 + 5	6.00 - 1	6.00 - 1	2.36 + 5
5	2.09306671 - 1	2.09306671 - 1	8.30979753 + 6	2.09 - 1	2.09 - 1	8.31 + 6
6	1.66690256 - 1	1.66690256 - 1	8.53997763 + 6	1.67 - 1	1.67 - 1	8.54 + 6
7	9.14942978 - 2	9.14942978 - 2	5.08538248 + 7	9.15 - 2	9.15 - 2	5.09 + 7
8	8.73673945 - 2	8.73673947 - 2	1.38782061 + 9	8.73 - 2	8.73 - 2	1.39 + 9
9	8.71466153 - 2	8.71466144 - 2	1.41042577 + 9	8.73 - 2	8.73 - 2	1.40 + 9
10	3.93514895 - 3	3.93514905 - 3	3.81499136 + 9	3.94 - 3	3.94 - 3	3.82 + 9
11	7.93411548 - 8	3.28110407 - 7	1.40706496 + 10	1.50 - 7	1.82 - 6	1.41 + 10
12	3.28744409 - 9	2.94899177 - 7	1.40738642 + 10	4.98 - 18	2.48 - 7	1.41 + 10
13	3.28744385 - 9	2.94772120 - 7	3.21019087 + 15	<b>2.03 - 7</b>	<b>2.03 - 7</b>	<b>1.00 + 0</b>
14	2.84586612 - 10	3.62878483 - 7	8.32790167 + 18	1.85 - 7	1.85 - 7	6.66 + 4
15	2.84586612 - 10	3.62900605 - 7	8.32790210 + 18	1.78 - 7	1.78 - 7	3.25 + 5
16	3.76425255 - 11	1.67507226 - 5	9.84930800 + 21	3.24 - 8	3.24 - 8	4.29 + 5
17	2.73041662 - 11	1.67328247 - 5	8.91283895 + 21	7.02 - 9	7.02 - 9	1.30 + 7
18	2.73041608 - 11	1.67581289 - 5	8.91305834 + 21	6.93 - 9	6.93 - 9	3.09 + 7
19	6.82351657 - 13	6.90349476 - 7	9.53171000 + 22	4.46 - 9	4.46 - 9	1.50 + 8
20	6.82351657 - 13	6.92385648 - 7	9.53179594 + 22	4.46 - 9	4.46 - 9	6.07 + 8
21	6.72452102 - 13	6.54577897 - 7	9.83975191 + 22	4.38 - 9	4.38 - 9	9.04 + 8
22	6.70811951 - 13	6.48248321 - 7	9.88983042 + 22	8.20 - 10	8.20 - 10	5.39 + 9
23	6.70811951 - 13	6.50677103 - 7	9.89048681 + 22	2.24 - 14	7.38 - 13	2.58 + 10
24	6.58769415 - 13	4.69784705 - 7	1.25798140 + 23	<b>7.37 - 13</b>	<b>1.01 - 12</b>	<b>1.00 + 0</b>
25	6.58769415 - 13	4.73672603 - 7	1.25802892 + 23	3.61 - 13	3.30 - 13	1.17 + 4
26	<b>4.70128524 - 7</b>	<b>4.70128328 - 7</b>	<b>1.00000000 + 0</b>	3.07 - 13	6.31 - 13	1.01 + 5
27	1.87736873 - 7	1.87736870 - 7	9.59415345 + 3	3.28 - 14	7.34 - 13	2.56 + 5
28	1.11797857 - 7	1.11797808 - 7	6.15064900 + 4	<b>7.33 - 13</b>	<b>6.52 - 13</b>	<b>1.00 + 0</b>
29	1.62744063 - 8	1.62744158 - 8	3.12694899 + 5	2.19 - 13	3.52 - 13	6.67 + 3
30	5.34499291 - 9	5.34499087 - 9	9.40826259 + 6	converged		
31	5.29674513 - 9	5.29674296 - 9	5.47342000 + 7			
32	3.54672002 - 9	3.54672030 - 9	2.69515192 + 8			
33	1.02373805 - 9	1.02370991 - 9	4.03740084 + 9			
34	9.69052509 - 10	9.69016629 - 10	1.23940329 + 10			
35	5.77211087 - 10	5.77211328 - 10	1.30139651 + 10			
36	8.28643039 - 14	6.05887230 - 13	2.72026861 + 10			
37	<b>6.05884655 - 13</b>	<b>6.04524129 - 13</b>	<b>1.00000000 + 0</b>			
38	4.30512161 - 14	2.45523317 - 13	2.43627507 + 3			

the average number of iterations in all cases, comparing  $m = 2$  and  $m = 6$ . As  $m$  grows, the execution time of smaller test problems decreases, since the cost of an extra iteration in a restart cycle is essentially the same as the cost of earlier ones and the later iterations sometimes contribute the most towards convergence as noted in [21]. For large problems ( $n = 1\,854$ ), the cost of the later added iterations becomes significant and increases CPU time (compare AGH:2 and AGH:4 for  $n = 1\,854$  in Table 4). Thus, some moderate value for  $m$  seems best for the proposed adaptive strategy.

It is clear from the data presented that AGMRES( $k$ ) outperforms both flexible GMRES( $\hat{k}$ ) and QMR. Since restarted flexible GMRES( $\hat{k}$ ) requires twice as much memory as restarted AGMRES( $k$ ), the restart value for FGS is taken as  $\hat{k} = k/2$ . Whenever FGS converges, it requires more work per iteration than AGH because a new preconditioner is computed at each FGS iteration. The QMR algorithm, subroutine DUQMR from QMRPACK [6], fails to find a solution with the required accuracy for any of the problems, but can solve some linear systems along the homotopy zero curve if the error tolerance is relaxed.

## 5. Conclusions

For applications requiring high accuracy linear system solutions, the adaptive GMRES( $k$ ) algorithm proposed here, which is based on Householder transformations and monitoring the GMRES convergence rate, outperforms several standard GMRES variants and QMR. The superiority is not in CPU time or memory requirements, but in robustness as a linear system solution ‘server’ for a much larger nonlinear analysis ‘client’ computation. The extra cost of Householder transformations is well justified by the improved reliability, and the adaptive strategy is well suited to the need to solve a sequence of linear systems of widely varying difficulty. In the context of large scale, multidisciplinary, nonlinear analysis it is hard to imagine not wanting the various components to be adaptive.

The high accuracy requirement causes types of failures in GMRES not usually seen in moderate accuracy uses of GMRES, and monitoring condition number estimates and the onset of stagnation within GMRES becomes crucial. Furthermore, ‘sanity’ checks (e.g., residual norm should be nonincreasing) within a GMRES algorithm must be modified for high accuracy. For instance, the limit on the number of iterations must be increased, and depending on other factors, an increasing residual norm may or may not dictate an abort (such details are in the pseudocode in Section 2). Finally, the three test problems are rather different, so the details of AGMRES( $k$ ) have not been tuned to one particular class of problems.

Future work should investigate a strategy for both increasing and decreasing the Krylov subspace dimension depending on measures of progress. Ideally the accuracy requested of the linear solver should match the accuracy actually required by the calling nonlinear analysis program, although in large scale computation it may be extremely difficult to estimate this minimum required accuracy.

## Acknowledgements

The authors gratefully acknowledge very helpful conversations with William McQuain and Robert Melville, and comments from the referees. The work of Sosonkina and Watson was supported in part by Department of Energy Grant DE-FG05-88ER25068, National Aeronautics and Space Administration Grant NAG-1-1562, National Science Foundation Grant DMS-9625968, and Air Force Office of Scientific Research Grants

F49620-92-J-0236 and F49620-96-1-0089. The work of Walker was supported in part by Department of Energy Grant DE-FG03-94ER25221 and National Science Foundation Grants DMS-9400217 and DMS-9727128.

## REFERENCES

1. C. H. Bischof and P. T. P. Tang. Robust incremental condition estimation. Tech. Rep. CS-91-133, LAPACK Working Note 33, Computer Science Department, University of Tennessee, May, 1991.
2. O. Axelsson and M. Nikolova. A generalized conjugate gradient minimum residual method (GCG-MR) with variable preconditioners and a relation between residuals of the GCG-MR and GCG-OR methods. *Comm. Appl. Anal.*, 1, 371–388, 1997.
3. Å. Björck. Solving linear least squares problems by Gram–Schmidt orthogonalization. *BIT*, 7, 1–21, 1967.
4. P. N. Brown and H. F. Walker. GMRES on (nearly) singular systems. *SIAM J. Matrix Anal. Appl.*, 18, 37–51, 1997.
5. C. DeSa, K. M. Irani, C. J. Ribbens, L. T. Watson and H. F. Walker. Preconditioned iterative methods for homotopy curve tracking. *SIAM J. Sci. Stat. Comput.*, 13, 30–46, 1992.
6. R. W. Freund and N. M. Nachtigal. An implementation of the look-ahead Lanczos algorithm for non-Hermitian matrices, part II. Tech. Rep. 90.46, RIACS, NASA Ames Research Center, November, 1990.
7. R. W. Freund and N. M. Nachtigal. QMR: a quasi-minimal residual method for non-Hermitian linear systems. *Numer. Math.*, 60, 315–339, 1991.
8. P. E. Gill and W. Murray. Newton-type methods for unconstrained and linearly constrained optimization. *Math. Programming*, 7, 311–350, 1974.
9. G. H. Golub and C. F. Van Loan. *Matrix Computations*, 2nd edition. Johns Hopkins University Press, Baltimore, MD, 1989.
10. A. Greenbaum, M. Rozložník and Z. Strakoš. Numerical behaviour of the modified Gram–Schmidt GMRES implementation. *BIT*, 37, 706–719, 1997.
11. S. M. Holzer, R. H. Plaut, A. E. Somers, Jr. and W. S. White. Stability of lattice structures under combined loads. *J. Engrg. Mech.*, 106, 289–305, 1980.
12. K. M. Irani, M. P. Kamat, C. J. Ribbens, H. F. Walker and L. T. Watson. Experiments with conjugate gradient algorithms for homotopy curve tracking. *SIAM J. Optim.*, 1, 222–251, 1991.
13. W. Joubert. On the convergence behavior of the restarted GMRES algorithm for solving non-symmetric linear systems. *Numer. Linear Algebra Appl.*, 1, 427–447, 1994.
14. R. K. Kapania and T. Y. Yang. Formulation of an imperfect quadrilateral doubly curved shell element for postbuckling analysis. *AIAA J.*, 24, 310–311, 1986.
15. W. D. McQuain, R. C. Melville, C. J. Ribbens and L. T. Watson. Preconditioned iterative methods for sparse linear algebra problems arising in circuit simulation. *Comput. Math. Appl.*, 27, 25–45, 1994.
16. R. C. Melville, S. Moinian, P. Feldmann and L. T. Watson. Sframe: an efficient system for detailed DC simulation of bipolar analog integrated circuits using continuation methods. *Analog Integrated Circuits Signal Processing*, 3, 163–180, 1993.
17. R. C. Melville, Lj. Trajković, S.-C. Fang and L. T. Watson. Artificial parameter homotopy methods for the DC operating point problem. *IEEE Trans. Computer-Aided Design*, 12, 861–877, 1993.
18. Y. Saad. A flexible inner–outer preconditioned GMRES algorithm. *SIAM J. Sci. Comput.*, 14, 461–469, 1993.
19. Y. Saad and M. H. Schultz. GMRES: a generalized minimal residual method for solving nonsymmetric linear systems. *SIAM J. Sci. Stat. Comput.*, 7, 856–869, 1986.
20. H. A. van der Vorst and C. Vuik. GMRESR: a family of nested GMRES methods. *Numer. Linear Algebra Appl.*, 1, 369–386, 1994.
21. H. A. van der Vorst and C. Vuik. The superlinear convergence behaviour of GMRES. *J. Comp. Appl. Math.*, 48, 327–341, 1993.
22. H. F. Walker. Implementation of the GMRES method using Householder transformations.

- SIAM J. Sci. Stat. Comput.*, 9, 152–163, 1988.
23. L. T. Watson. Globally convergent homotopy methods: a tutorial. *Appl. Math. Comput.*, 31BK, 369–396, 1989.
  24. L. T. Watson, S. M. Holzer and M. C. Hansen. Tracking nonlinear equilibrium paths by a homotopy method. *Nonlinear Anal.*, 7, 1271–1282, 1983.
  25. L. T. Watson, S. C. Billups and A. P. Morgan. Algorithm 652: HOMPACT: a suite of codes for globally convergent homotopy algorithms. *ACM Trans. Math. Software.*, 13, 281–310, 1987.
  26. T. Y. Yang, R. K. Kapania and S. Saigal. Accurate rigid-body modes representation for a nonlinear curved thin-shell element. *AIAA J.* 27, 211–218, 1989.